JPSE (Journal of Physical Science and Engineering), Vol. 8, No. 1, 2023, Page 36–51.
DOI: 10.17977/um024v8i12023p036

JPSE
(Journal of Physical Science and Engineering)

http://journal2.um.ac.id/index.php/jpse
EISSN: 2541-2485

Automatic Excitation Control Using PI Method Based on Analysis Root Locus for Synchronous Generator

Received
26 September 2021

Revised
23 December 2022

Accepted for Publication
01 May 2023

Published
24 July 2023

A M Ravi* and A T Nugraha[1]

Department of Marine Electrical Engineering, Shipbuilding Institute of Polytechnic Surabaya, Jl. Teknik Kimia Keputih Sukolilo, Surabaya, 60111, Indonesia.

***E-mail:** muhammad.alwy.ravi@gmail.com

Abstract
The demand for electrical energy is increasing (at 2–3% per year). It is necessary to utilize the energy available in nature optimally and stably to fulfill electricity needs. Synchronous generators have an essential role in fulfilling electricity needs. Maintaining and improving the operational stability of the synchronous generator is fundamental to the safe and economical operation of an electric power system. The use of control methods to increase control excitation is recognized as an economical and effective way. Previous research shows there are still areas for improvement in the excitation control method. Thus, this research focuses on optimizing the automatic excitation system using the PI control method with stability analysis using the root locus. The effect of PI control on the results of the characteristics response has T_r = 1.9 s, T_s = 6.6 s, M_p = 38.95%, and E_{ss} = 11.02%. While the generator excitation current will increase in line with the increase in load current, and the resulting output voltage will be stable with errors that occur when compared to the nominal voltage is 10.51% because the sensor reading is affected by a frequency that is not following the operating frequency.
Keywords: Synchronous generator, PI control, excitation system, root locus.

1. Introduction

The demand for electrical energy, along with the times, is increasing, with more requests than other energies [1]. The demand for electrical energy is increasing (at 2–3% per year) [2]. It is necessary to utilize the energy available in nature optimally and stably to fulfill the demand for electrical energy. Utilization of available energy in nature is carried out through an energy conversion process from potential energy to mechanical energy, which is then converted into electrical energy by a synchronous generator. The synchronous generator is defined as a machine that transfers energy from mechanical to electrical [3]. Maintaining and improving the operational stability of the synchronous generator is fundamental to the safe and economical operation of the electric power system. Of the many measures to improve the stable operation of synchronous generators, using control methods to increase control excitation is recognized as an economical and effective way [4].

Jiang [5], in his research, discusses the excitation system of a synchronous generator using PID (Proportional Integral Derivative) control as an excitation control method. Tests in this journal are carried out through simulations with MATLAB and comparing simulations of open-loop control systems with closed-loop control systems using the PID control method. The test results show that PID control is better than open-loop control in setting time, rise time, and overshoot. The drawback of this study is that it only performs testing through simulation and compares two parameters in excitation control when there is a loading effect.

Another research by Bhutto [6] discusses the design and implementation of AVR (Automatic Voltage Regulator) based on PNN (Probabilistic Neural Network) to increase the transient stability limit of the power system. In this study, controlling and achieving stability and consistency in active and reactive power was designed using a PNN controller in the MATLAB neural network toolbox. Before PNN was implemented, a conventional PID controller was implemented in MATLAB, where the AVR response values were taken satisfactorily as input and training data for PNN. The conventional PID parameters used to generate this new neural network were obtained from Ziegler-Nichols's analysis

method. The results of this study indicate the ability of PNN-based AVR to have better transient stability limits under various loading conditions. The weakness of this research is that the analysis of the determination of PID parameters is still using the Ziegler-Nichols Oscillation Method. Hence, the resulting analysis needs to know the limits of system stability in determining the new neural network. Pribadi [7], in his research, discusses optimizing a voltage stabilizer system using a choke converter type converter with the PI (Proportional Integral) control method. The PI control method implemented on the choke converter as an exciter produces an excellent response to the resulting generator output voltage. The system modeling in this study uses PSIM software for excitation control. The drawback of this study is that it only uses PSIM software as a test through simulation, and there is no direct application of the tool.

Based on the description of previous similar research on synchronous generator excitation control, some things could still be improved. The disadvantages of this previous research are used as the fundamental basis for the focus of research development in this journal. The focus of development in this research is optimizing the automatic excitation system using the PI control method with stability analysis using the root locus to determine the PI parameters on the synchronous generator. The root locus analysis used in this study uses MATLAB to see the system stability response curve directly so that it can quickly determine the stability limit of the system. The main goal to be achieved in this research is to produce an automatic excitation control system reference if applied directly. So, this research is expected to impact the design of a synchronous generator voltage stabilizer prototype that responds well to load changes.

2. Method

2.1. Excitation System

The excitation current is provided by an excitation system consisting of an AVR, exciter, measuring element, power system stabilizer (PSS), and limiting and protection unit [8]. The exciter in the excitation system will supply direct current electricity as a reinforcement to the electric generator so that it produces electric power and the output voltage depends on the amount of excitation current [9]. The generator excitation system is essential to form a stable generator terminal voltage [10]. The design of the excitation system is shown in Figure 1.

The excitation system is classified according to the strengthening of the excitation power into three types: the DC (Direct Current) excitation system, the AC (Alternating Current) excitation system, and the static excitation system [3]. This research focuses on a DC excitation system that provides a field current to be applied to the rotating part coil of a synchronous machine directly through the slip-ring. The DC excitation system used is its amplifier by rectifying the output voltage of the synchronous generator. It is then stored in the battery and used as a supply to the exciter, namely the buck-boost converter.

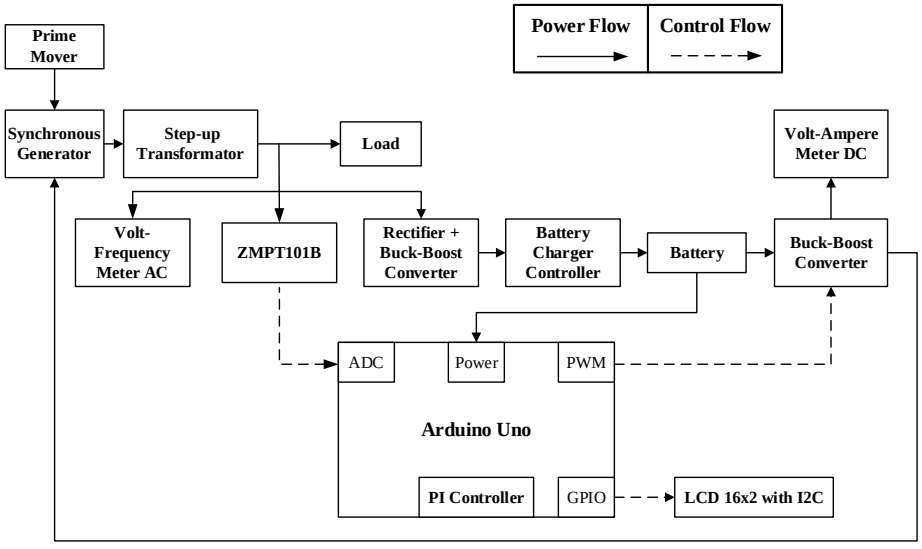

Figure 1. Block diagram system.

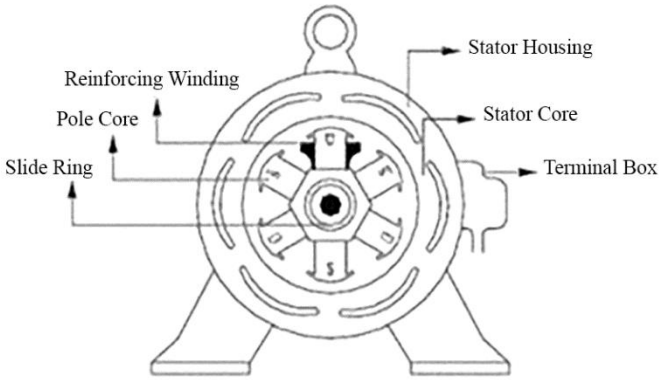

Figure 2. A simple construction of synchronous generator [11].

2.2. Synchronous Generator

An AC generator, or called an alternator, is a piece of equipment that functions to convert mechanical energy (motion) into electrical energy (electricity) through magnetic field induction. This energy change occurs due to a change in the magnetic field in the armature coil (where the voltage is generated in the generator). It is said to be a synchronous generator because the number of rotations of the rotor is equal to the number of rotations of the magnetic field on the stator [9]. This synchronous speed results from the rotational speed of the rotor, with the magnetic poles rotating at the same speed as the rotating field on the stator. The field coil in the synchronous generator is located on the rotor, while the armature coil is on the stator [2]. A simplified form of a synchronous generator is shown in Figure 2.

The synchronous generator consists of two essential elements: stator and rotor. The stator is part of the stationary synchronous generator, where the induced voltage is generated. At the same time, the rotor is part of a synchronous generator that moves and is supplied with direct current in the coil. The magnitude of the induced voltage generated in the stator phase is obtained from Equation 1.

$$E_A = K \times \Phi \times \omega \tag{1}$$

This output voltage depends on the flux Φ in the machine, the rotational speed ω and the construction of the machine which is represented by the constant K [12].

2.3. Control Method

The control design in this study aims to adjust the excitation value as a generator output voltage stabilizer under the needs of the magnetic field on the synchronous generator. The control design used in optimizing the automatic excitation system uses the PI control method with stability analysis using the root locus to determine the PI parameters on the synchronous generator. The PI control method in the design will also be compared with the P and PID control methods in the Simulink MATLAB simulation and applied directly to the tool. The comparison results will get the best control method to be applied to the tool when there is a change in electrical load.

PID controller is a controller to determine the precision of an instrumentation system with the characteristics of the feedback on the system. PID components consist of three types: proportional, integrative, and derivative. All three can be used together or separately, depending on the response we want to a plant [13]. PID is a control method with an excellent mathematical model because the error can be changed to near zero, and stability control can be achieved by equating the process variable value with the setpoint value [14]. The definition of PID (t) is as a control output, while as a standard, the PID algorithm can be formulated according to Equation 2,

$$u(t) = K_p e(t) + K_i \int_0^t e(\tau)dt + K_d \frac{d}{dt} e(t) \tag{2}$$

where $e(t)$ is the input signal while $u(t)$ is the PID response output signal.

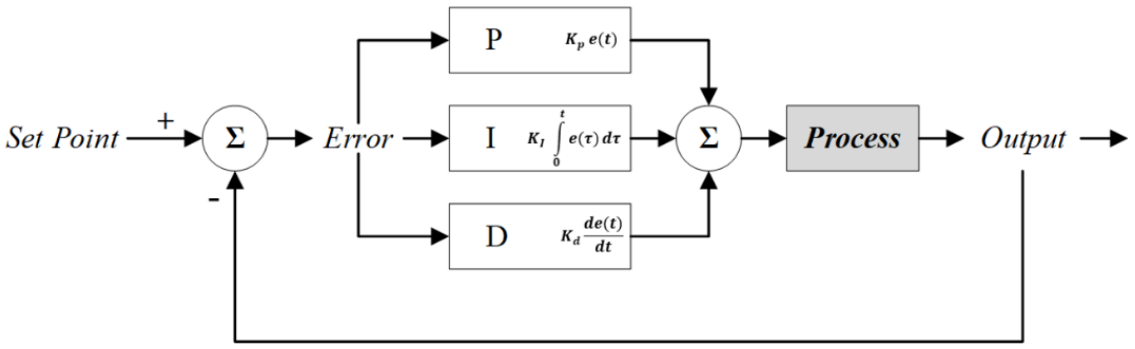

Figure 3. The block diagram of P, PI, and PID control [15].

Based on Equation 2, the PID control will be obtained in the form of a transfer function according to Equation 3 [16]. Equation 3 will be used to find the value of the gain P, I, and D so that the parameters of each control method will be compared. Figure 3 is a P, PI, and PID control block diagram.

$$G_c(s) = K_p\left(1 + \frac{1}{T_i s} + T_d s\right) \tag{3}$$

2.4. System Identification MATLAB

Due to the increasing demand for fault detection, monitoring, and predictive maintenance, online or recursive identification plays a more critical role in systems engineering. In the latest release of System Identification ToolboxTM for MATLAB, this has been reflected in more substantial support for online techniques. This contribution sheds light on this increase [17]. System identification is concerned with building a mathematical model of a dynamic system based on the measurement of input and output signals. There are four crucial decisions in the system identification problem [18]. First, designing experiments and collecting data. Second, deciding on the structure of the model. Third, estimate the parameters of the model structure by adjusting it to the data. Fourth, validation of the model.

In this study, the natural response characteristic data was taken from the plan first as input-output data on the system Identification. The natural response of the plan can be determined by sampling the output voltage response data on the Arduino serial monitor. The sampling data on the serial monitor used is the result of reading for 20 seconds from the voltage sensor. The output voltage value (as the system identification output) is the response value that occurs due to the provision of excitation (as the system identification input) on the synchronous generator. The input-output data is estimated using the continuous-time identified TFEST (Transfer Function Estimation) on the time domain data [19]. After the identification process, we obtain the transfer function of the parameterization and status as Table 1. Functions the transfer of the estimation results will then be simulated to see the resulting response when the system is still in the OLTF (Open-Loop Transfer Function) condition. The system OLTF simulation is done by providing step input to the system. Figure 4 is an OLTF block diagram with a step input.

Table 1. The transfer function of the parameterization and status.

Parameterization	Status
Number of poles	4
Number of zero	0
Number of free coefficients	5
Fit to estimation	91.13%
Final prediction error (FPE)	45.57
Mean-square error (MSE)	18.23

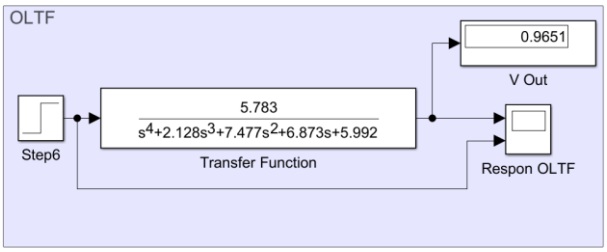

Figure 4. Open loop transfer function.

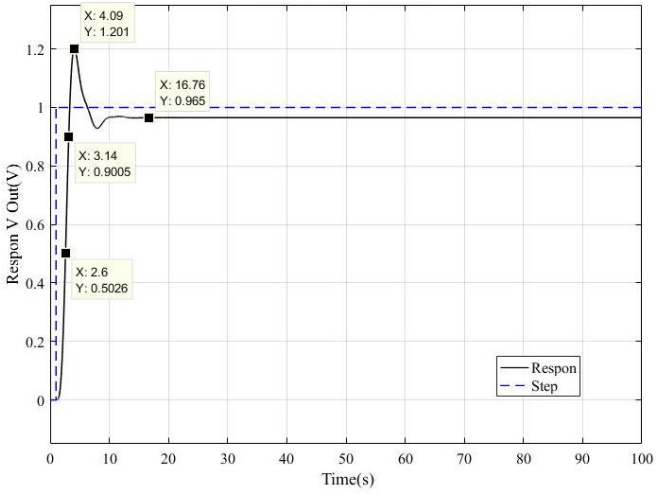

Figure 5. Open loop transfer function response curve.

From the modeling results, if simulated with an input step, it will produce a response according to Figure 5. The resulting steady-state error is 3.49%, the rise time is 3.14 seconds, the maximum overshoot is 20.1%, and the settling time is 16.76 seconds. Before the natural response control method, the system had a high overshoot value.

2.5. Root Locus Analysis

The closed-loop poles determine the essential characteristics of the transient response of a closed-loop system. In analytical problems, we need to determine the locations of closed-loop poles in the *S* plane. The closed-loop poles are the roots of the characteristic equation. It is necessary to describe the characteristic polynomial of its factors [20]. The characteristic equation obtained in this study has a polynomial degree of more than three, so finding closed-loop roots in this research plan is challenging. The MATLAB tool makes finding the roots of the characteristic equations obtained easier. MATLAB has an application called control system designer that can be used to design linear control systems [20]. In this application, we can quickly determine P, PI, and PID parameters using root locus analysis by shifting the poles on the boundary of the imaginary axis (poles are on the LHP (Left Half Plane)) to make the system have a stable response. The characteristic response designs made are (T_r < 5 s), (M_p < 5%), (T_s < 12 s), and (E_{ss} < 2%).

2.5.1. Root Locus Analysis for Proportional Gain Control

Determination of the proportional amplifier value is done by shifting the pole value along the locus (root locus) to obtain a gain or amplifier value that considers the LHP and RHP (Right Half Plane) values on the real axis and imaginary axis. A system will be stable if it has roots in the LHP section to the left of the imaginary axis. Figure 6 below shows the amplifier value's determination using the proportional method. Figure 6 shows the root locus of the modeling transfer function, which can be shifted by the root value to obtain a proportional gain value with a stable system state. The proportional gain (K_p) from the pole shift at the locus is 1.118.

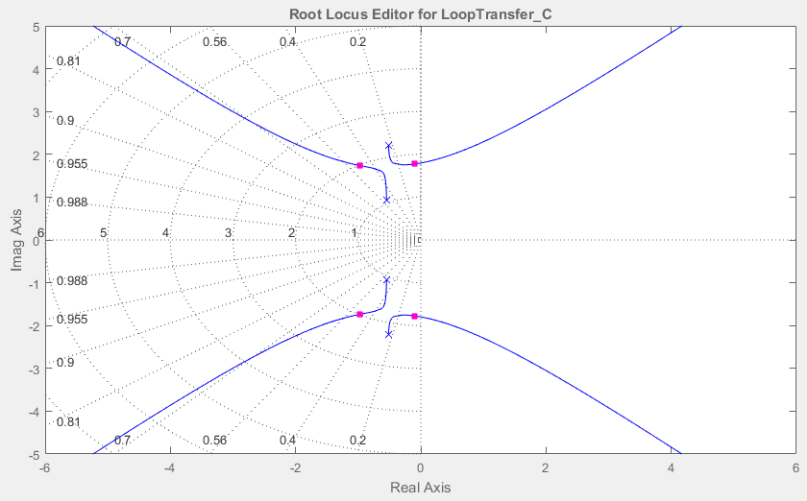

Figure 6. Proportional (P) pole with root locus.

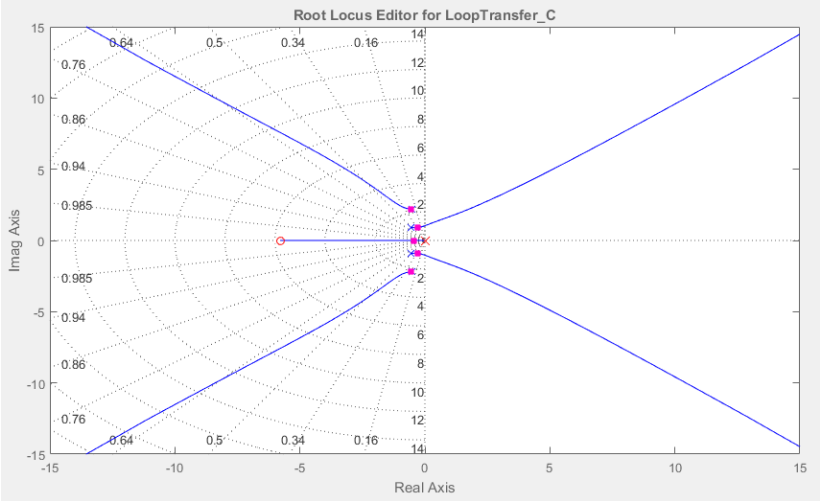

Figure 7. Proportional-integral (PI) pole with root locus.

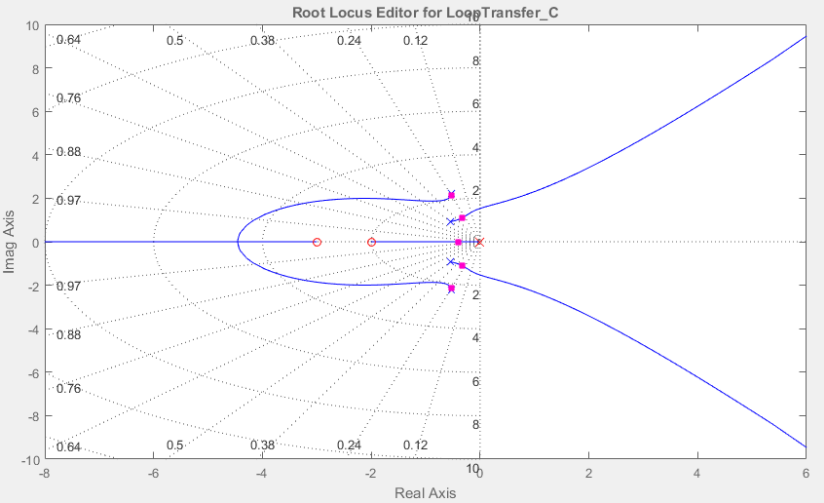

Figure 8. Proportional-integral-derivative (PID) pole with root locus.

2.5.2. Root Locus Analysis for Proportional and Integral Gain Control

The proportional integral control gain using the root locus method can be obtained by adding the integrator and absolute zero to the C (compensator) value in the control system designer. The addition of the integrator and absolute zero values is under the type of method used, which produces the PI control method equation. From the equation of the control method, a root locus graph for the PI control will be obtained, as shown in Figure 7. The position of the roots in Figure 7 produces a gain control for PI of K_p is 0.062 and K_i is 0.3585. This gain value will be used for simulation on Simulink MATLAB. The simulation is carried out to obtain the system response characteristics with PI control.

2.5.3. Root Locus Analysis for Proportional Integral Derivative Gain Control

Proportional integral derivative control with the root locus method can be found for the strengthening value of K_p, K_i, and K_d by adding an integrator, real zero-1, and real zero-2 in the compensator editor. The addition is under Equation 3 in the form of the transfer function. Adding the integrator, real zero-1, and real zero-2 will produce a root locus editor graph, as shown in Figure 8. The root locus graph in Figure 8 determines the strengthening value of K_p, K_i, and K_d by shifting the pole on the LHP to the left of the imaginary axis. Based on the graph in Figure 8, the K_p value is 0.365, K_i is 0.438, and K_d is 0.073 obtained.

3. Result and Discussion

The tests carried out in this study consisted of simulations on Simulink MATLAB and direct testing on the alternator. The control methods simulated and implemented on the device are the P, PI, and PID. Response data from the three methods will be compared to show the best method that can be applied to the alternator.

3.1. P Control Simulation

The block diagram of the control system with the proportional control method is shown in Figure 9. The proportional gain used is 1.118, according to the root locus analysis performed. The simulation results from the block diagram in Figure 9 are the response curves shown in Figure 10. Then the response curve will be compared with the results of the PI and PID methods.

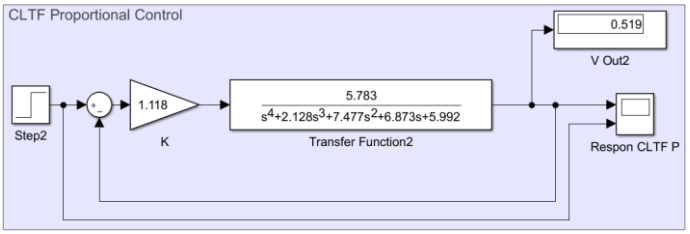

Figure 9. Closed-loop control system diagram with P control.

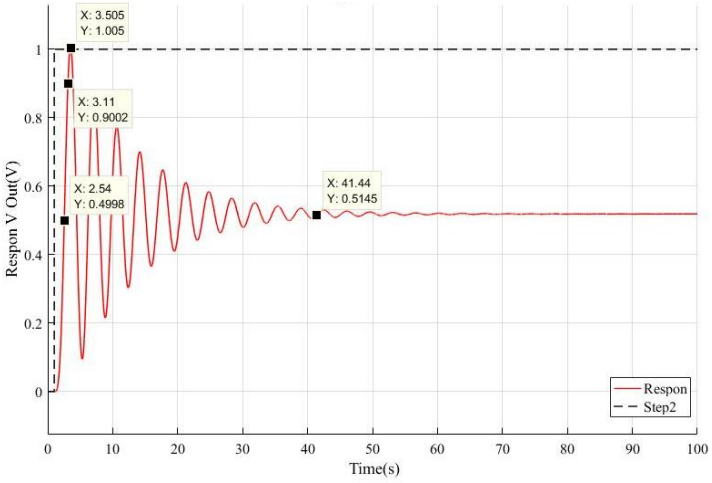

Figure 10. Response curve with P control.

The response curve with proportional control produces an oscillating characteristic with a settling time (T_s) of 41.44 s at an amplitude of 0.5145. The response that oscillates for 41.44 seconds will cause the voltage stabilizer plan to be unable to stabilize the resulting voltage. The steady-state error (E_{ss}) value generated by this proportional control response to the setpoint is 48.55%, which is unsuitable when applied.

3.2. PI Control Simulation

The block diagram of the system with PI control in the simulation, using K_p = 0.062 and K_i = 0.3585 according to the root locus analysis performed. Simulation of this PI control method is done by providing step input. The response results from this control will be compared with the setpoint to determine the resulting characteristics. Figure 11 is a block diagram of a system with PI control simulated using Simulink MATLAB. Simulation for this PI control method produces a response curve, as shown in Figure 12, which has good response characteristics with the values shown in Table 2. The resulting response characteristics are good without any steady-state error and have a slight overshoot following the expected design.

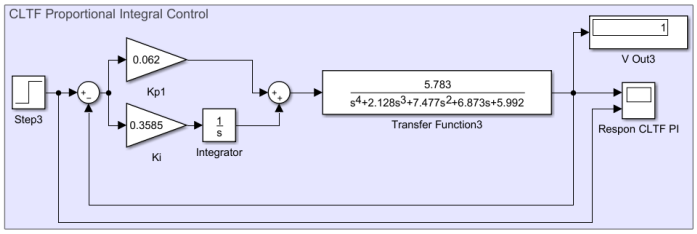

Figure 11. Closed-loop control system diagram with PI control.

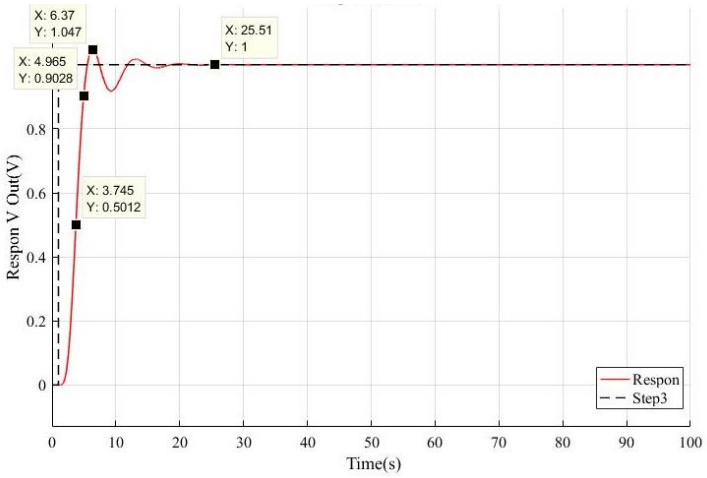

Figure 12. Response curve with PI control.

Table 2. The transfer function of the parameterization from PI control simulation.

Characteristic	Value
Delay time (T_d)	3.745 s
Rise time (T_r)	4.965 s
Time peak (T_p)	6.370 s
Settling time (T_s)	25.510 s
Delay output (Y_d)	0.5012 V
Rise output (Y_r)	0.9028 V
Ouput peak (Y_p)	1.0470 V
Settling output (Y_s)	1.0000 V
Maximum overshoot (M_p)	4.7%
Error steady-state (E_{ss})	0.0%

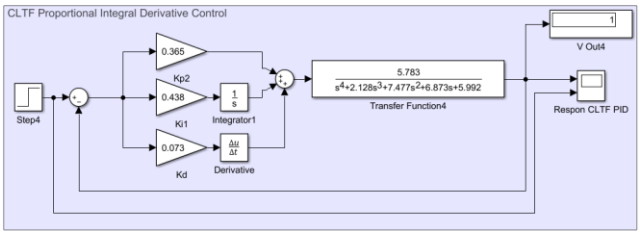

Figure 13. Closed-loop control system diagram with PID control.

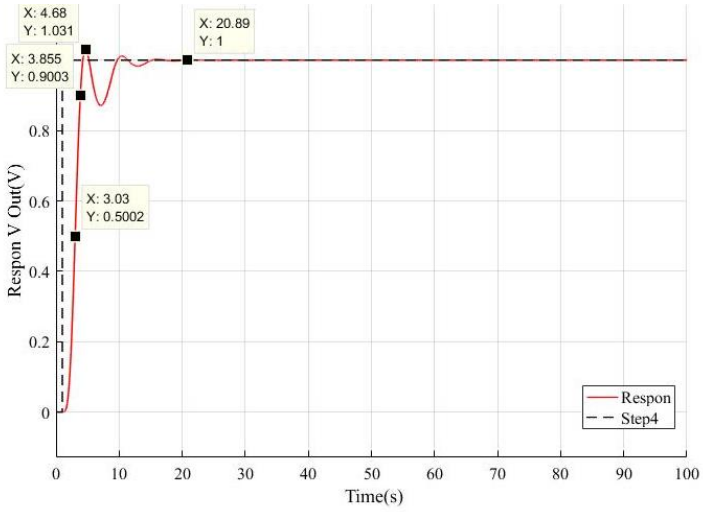

Figure 14. Response curve with PID control.

Table 3. The transfer function of the parameterization from PID control simulation.

Characteristic	Value
Delay time (T_d)	3.030 s
Rise time (T_r)	3.855 s
Time peak (T_p)	4.680 s
Settling time (T_s)	20.890 s
Delay output (Y_d)	0.5002 V
Rise output (Y_r)	0.9003 V
Ouput peak (Y_p)	1.0310 V
Settling output (Y_s)	1.0000 V
Maximum overshoot (M_p)	3.1%
Error steady-state (E_{ss})	0.0%

3.3. PID Control Simulation

The proportional integral derivative method in this system simulation can be seen in the block diagram in Figure 13. The respective gain for this PID are, $K_p = 0.365$, $K_i = 0.438$, and $K_d = 0.073$. The simulation is carried out by providing the input step as a set point. Figure 14 is the response curve of block diagram simulation results with PID control. The response curve has the characteristics of the plan if there is a PID control, including system response curve when given PID control has a better response compared to P and PI. However, the good simulation results will also be compared with the results of direct application to the alternator to determine the best control method for the generator output voltage stabilizer system in this study.

3.4. Comparison of Response Characteristics of Simulation Control Methods

Comparison of the control methods in this plan has the aim of clearly knowing the difference between each control method when applied to the plan during the simulation. Figure 15 is the response curve of the system compared with the three methods (P, PI, and PID). The characteristics of each application

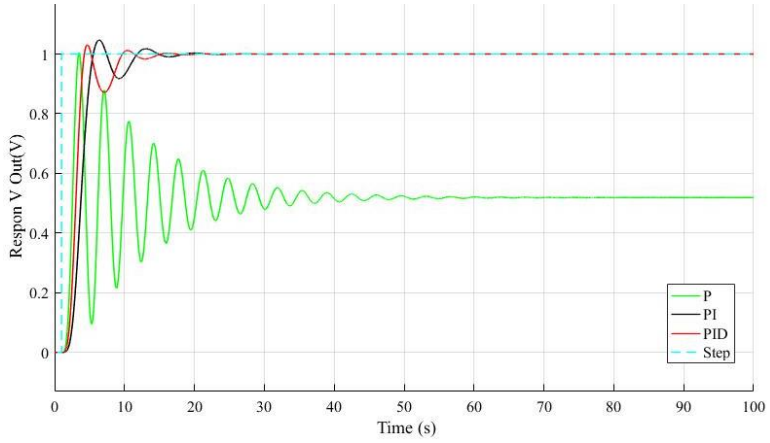

Figure 15. Comparative response curves of P, PI, and PID methods.

Table 4. Comparison of response characteristics.

Characteristics Response	P	PI	PID
Delay time (T_d)	Oscillation (2.540 s)	3.745 s	3.030 s
Rise time (T_r)	Oscillation (3.110 s)	4.965 s	3.855 s
Time peak (T_p)	Oscillation (3.505 s)	6.370 s	4.680 s
Settling time (T_s)	41.440 s	25.510 s	20.890 s
Maximum overshoot (M_p)	Oscillation	4.7 %	3.1 %
Error steady-state (E_{ss})	48.55 %	0 %	0 %

of the control method in Figure 15 can be seen from the differences between each control method in Table 4. Table 4 contains data on the comparison of response characteristics to the control method used. The response that has good characteristics from the three is the PI control method with a fairly low overshoot value, no steady-state error and a smaller undershoot when compared to the PID control.

3.5. The Implementation of P Control for Characteristics Response

Control with this proportional method utilizes the gain value of the system simulation test results, namely K_p = 1.118. The test results obtained the response characteristic curve according to Figure 16. The response characteristics of the system with proportional control show that the system is oscillating and unstable. Table 5 contains the value of the system response characteristics with proportional control according to the response curve obtained.

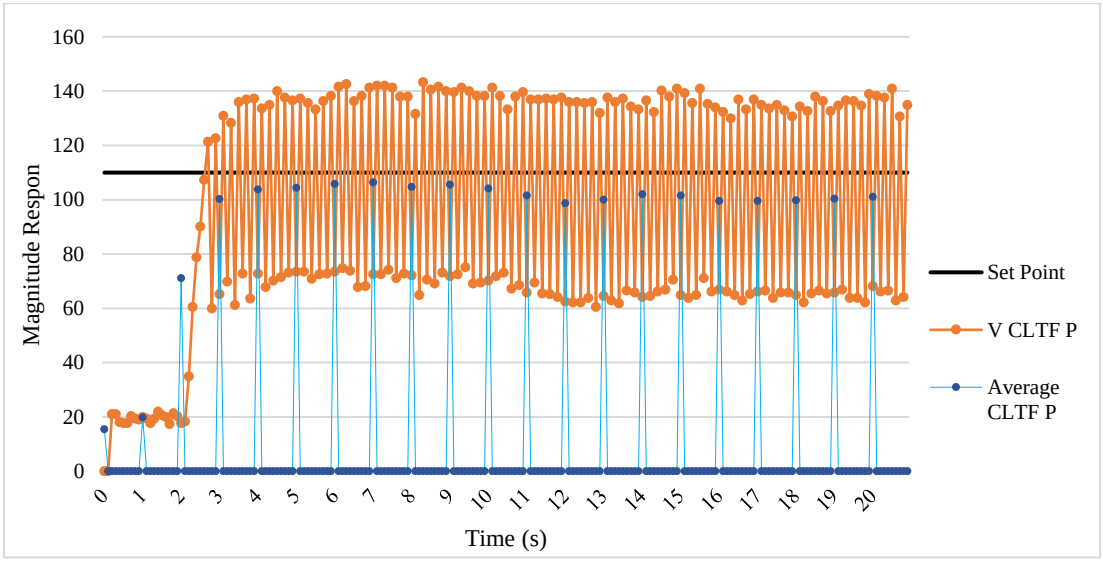

Figure 16. The output voltage response curve with P control.

Table 5. Characteristics response of closed-loop control system with P control method.

Characteristics Response	Magnitude	Unit
V_f (excitation voltage)	Oscillation	V
I_f (excitation current)	Oscillation	A
n_r (rotating speed)	1342	RPM
f (frequency)	179.9	Hz
T_d (delay time)	2.4	s
T_r (rise time)	2.6	s
T_p (peak time)	Oscillation	s
T_s (settling time)	Oscillation	s
M_p (maximum overshoot)	Oscillation	%
E_{ss} (error steady-state)	Oscillation	%

Response characteristics data in Table 5 indicate that the system is oscillating and unstable. This oscillating response makes the excitation value for the generator fluctuate which causes the output voltage to become unstable.

3.6. The Implementation of PI Control for Characteristics Response

Closed-loop control with this proportional-integral method using gain values of K_p and K_i are 0.062 and 0.3585, respectively. The test results with the PI method are shown in Figure 17. The response curve shows that the output voltage response is stable. The description of each response characteristic value of the curve is shown in Table 6.

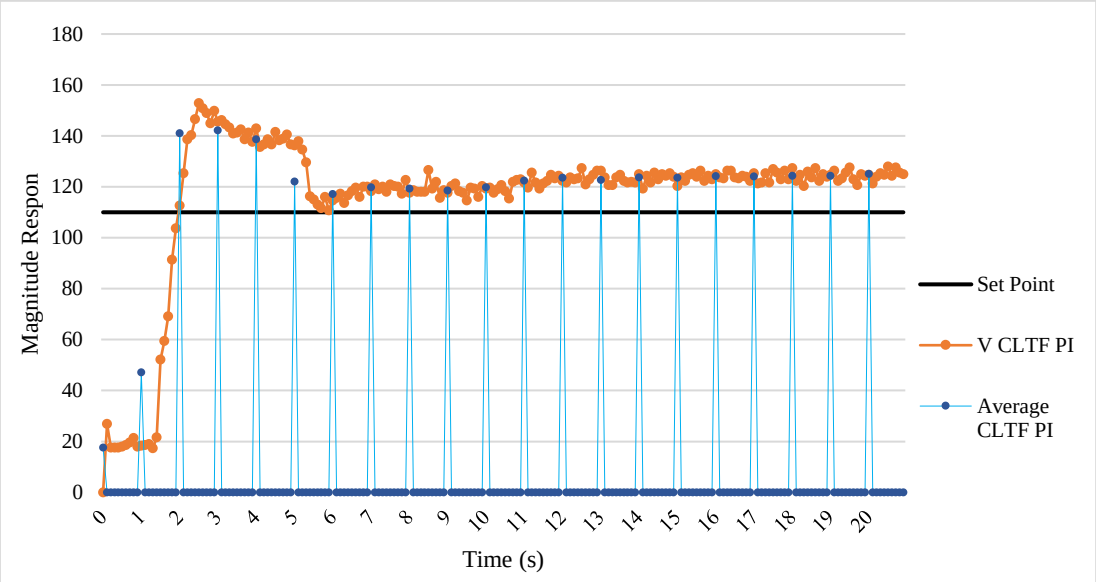

Figure 17. The output voltage response curve with PI control.

Table 6. Characteristics response of closed-loop control system with PI control method.

Characteristics Response	Magnitude	Unit
V_f (excitation voltage)	15.0	V
I_f (excitation current)	0.66	A
n_r (rotating speed)	1256	RPM
f (frequency)	165.3	Hz
T_d (delay time)	1.6	s
T_r (rise time)	1.9	s
T_p (peak time)	2.6	s
T_s (settling time)	6.6	s
M_p (maximum overshoot)	38.95	%
E_{ss} (error steady-state)	11.02	%

Response of the system when using the PI control will produce a good response marked by the stable generator output voltage. The output voltage response will reach 90% of the setpoint within 1.9 seconds, with a small steady-state error of 11.02%. The steady-state error value of more than 5% is caused because the sensor has a reading error with the display meter of 14.36%. Behind the error value, which is still relatively large, the response follows the expected design for the values of T_r (rise time) and T_s (settling time).

3.7. The Implementation of PID Control for Characteristics Response

Closed-loop control testing using the PID method is still carried out even though it has received a good response from the PI control in the previous test. This test aims to see whether the resulting response is better than the response with the PI control. The characteristics of the test response using the PID method can be seen in Figure 18.

The PID method test results produce a response that has been oscillating from the beginning and the oscillations are getting bigger starting in the period between 2–3 seconds. The resulting response does not match the simulation results. The characteristics of the response using the PID method are shown in Table 7. Response of the system using the PID control method causes the output voltage value to be unstable. The initial response oscillating is not good when applied in the tool.

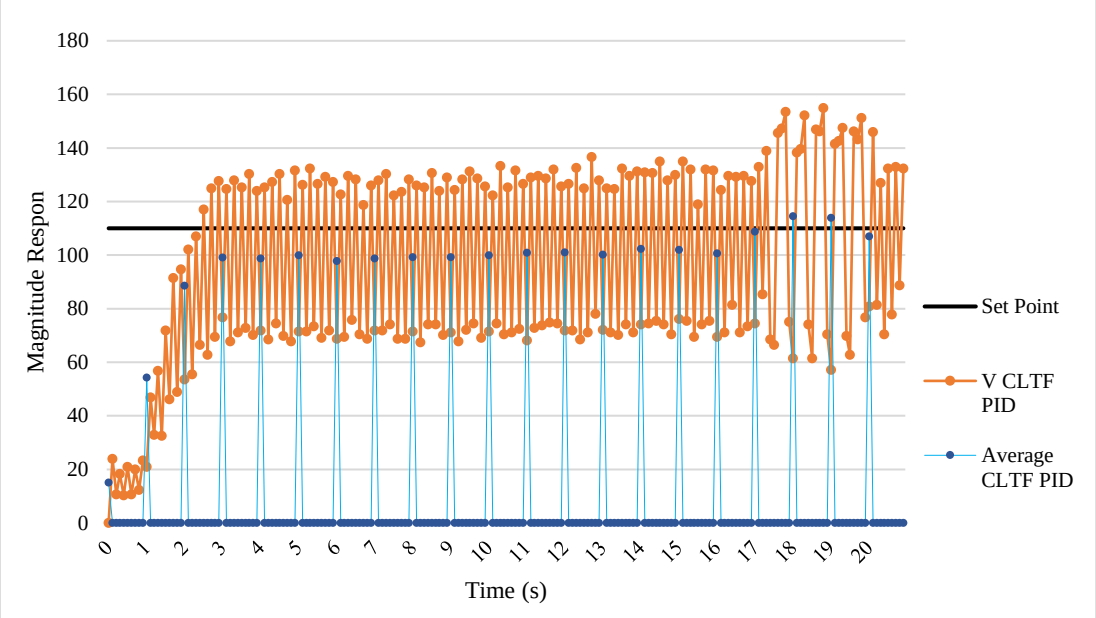

Figure 18. The output voltage response curve with PID control.

Table 7. Characteristics response of closed-loop control system with PID control method.

Characteristics Response	Magnitude	Unit
V_f (excitation voltage)	Oscillation	V
I_f (excitation current)	Oscillation	A
n_r (rotating speed)	1350	RPM
f (frequency)	177.5	Hz
T_d (delay time)	Oscillation	s
T_r (rise time)	Oscillation	s
T_p (peak time)	Oscillation	s
T_s (settling time)	Oscillation	s
M_p (maximum overshoot)	Oscillation	%
E_{ss} (error steady-state)	Oscillation	%

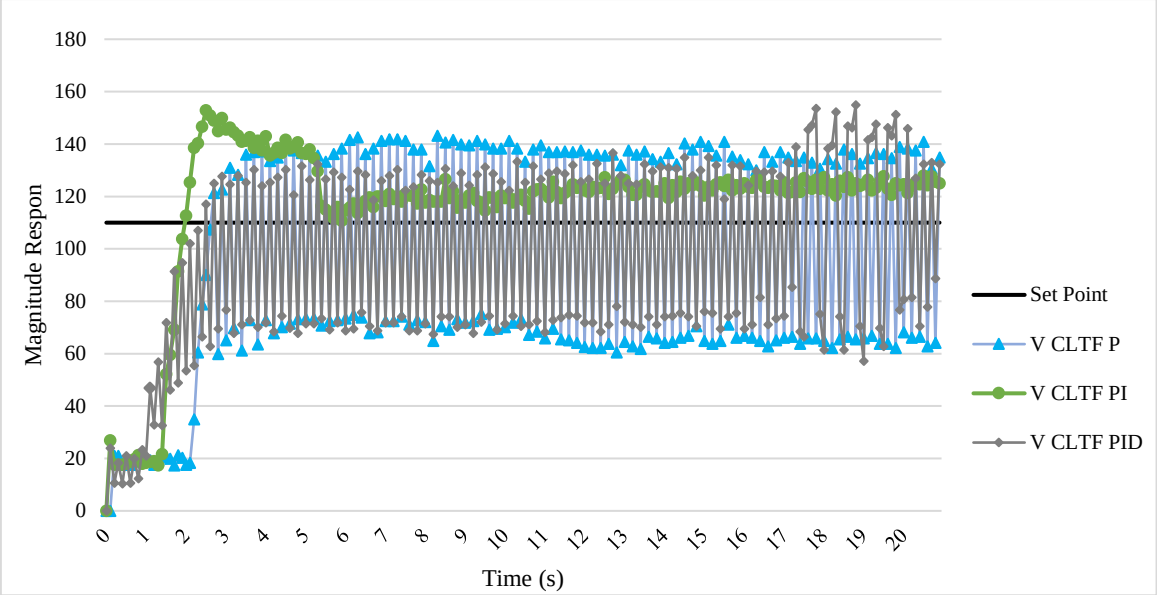

Figure 19. Comparison of the output voltage response curve.

Table 8. Comparison of the characteristics response curve.

Characteristics Response	Magnitude			Unit
	P	PI	PID	
T_d (delay time)	2.4	1.6	Oscillation	s
T_r (rise time)	2.6	1.9	Oscillation	s
T_p (peak time)	Oscillation	2.6	Oscillation	s
T_s (settling time)	Oscillation	6.6	Oscillation	s
M_p (maximum overshoot)	Oscillation	38.95	Oscillation	%
E_{ss} (error steady-state)	Oscillation	11.02	Oscillation	%

3.8. Comparison of Response Characteristics Using Control Methods

The response characteristics of several control methods used will be compared to obtain the best response value to be applied in the plan. The comparison of these responses is shown in Figure 19 below. Comparison between the response characteristics of each control method in Table 8 shows that if applied in the plan, the PI control method will produce a good response with a maximum overshoot of 38.95% and a steady-state error of 11.02%.

3.9. Comparison Between Simulation and Implementing PI Control

The result data in Table 9 is the overall difference in the response characteristics of the PI control type data compared to the simulation data. In the table, the response between the test and simulation data has a difference for the time response in the test is faster than the simulation, while for M_p (%) and E_{ss} (%), it is greater than the simulation.

Table 9. Comparison between simulation testing and implementation testing with PI control.

Characteristics Response	Magnitude		Unit	Response
	Simulation Testing	Implementation Testing		
T_d (delay time)	3.745	1.6	s	Faster
T_r (rise time)	4.965	1.9	s	Faster
T_p (peak time)	6.370	2.6	s	Faster
T_s (settling time)	25.510	6.6	s	Faster
M_p (maximum overshoot)	4.7	38.95	%	Greater
E_{ss} (error steady-state)	0	11.02	%	Greater

3.10. Automatic Excitation Testing with the Best Control Method (PI)

Testing of the plan using the best control method is carried out after obtaining a method with good response characteristics to be applied. The best control method applied in this plan is a closed-loop control system with the PI method. The test results with the best control method are shown in Table 10, where E1 is sensor error to display, E2 is error reading to setpoint, D is display, and S is sensor.

The test data in Table 10 can be illustrated in Figure 20 and Figure 21. The graphs in Figure 20 illustrate the effect of the adding load value by an increase in load current on the excitation current. In contrast, the graph in Figure 21 illustrates the effect of increasing the excitation current value on the output voltage and frequency under load conditions by applying the PI control to the plan made. The PI control applied in the tool in this study, as shown in Figure 21, influences the voltage value that will be stable at a voltage nominal working 110 VAC under changing load conditions. The controlled excitation current causes this stable voltage under the load changes in Figure 20.

Table 10. Load testing data with the best control method.

n_r (RPM)	V_f (V)	I_f (A)	PWM	f (Hz)	$V_{display}$ (V)	V_{sensor} (V)	Type of Load	I_a (mA)	E1 (%)	E2 (%)	
										D	S
1189.00	16.20	0.71	44	168.10	106.00	110.00	3 watt LED	34.00	3.77	3.64	0.00
1164.00	16.40	0.72	26	162.50	99.00	109.90	5 watt LED	63.00	11.01	10,00	0.09
1110.00	20.10	0.88	9	154.10	104.00	112.20	10 watt LED	95.00	7.88	5,45	2.00
990.80	23.00	1.04	9	152.20	120.00	145.20	20 watt LED	80.00	21.00	9,09	32.00
985.30	20.10	0.88	-19	137.50	70.00	89.70	5 watt lampu pijar	150.00	28.14	36,36	18.45
Average Error (%)									14.36	12.91	10.51

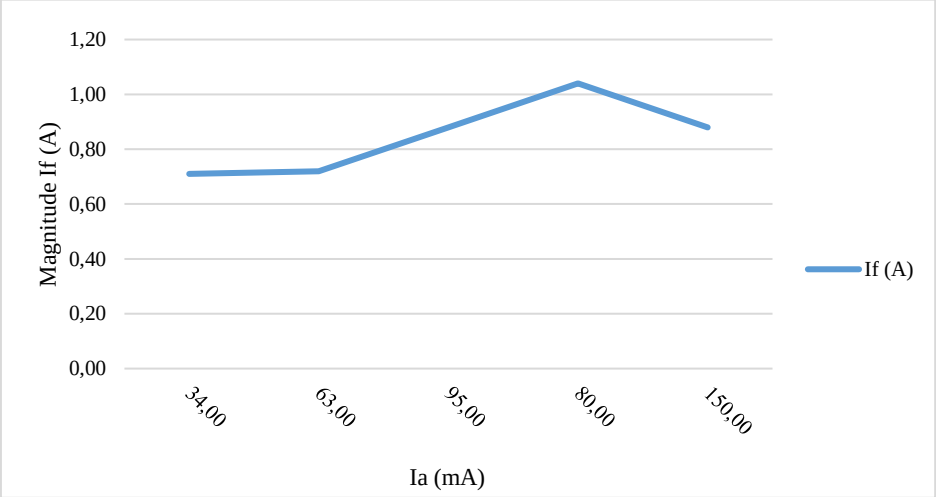

Figure 20. Graph of the effect I_a against I_f.

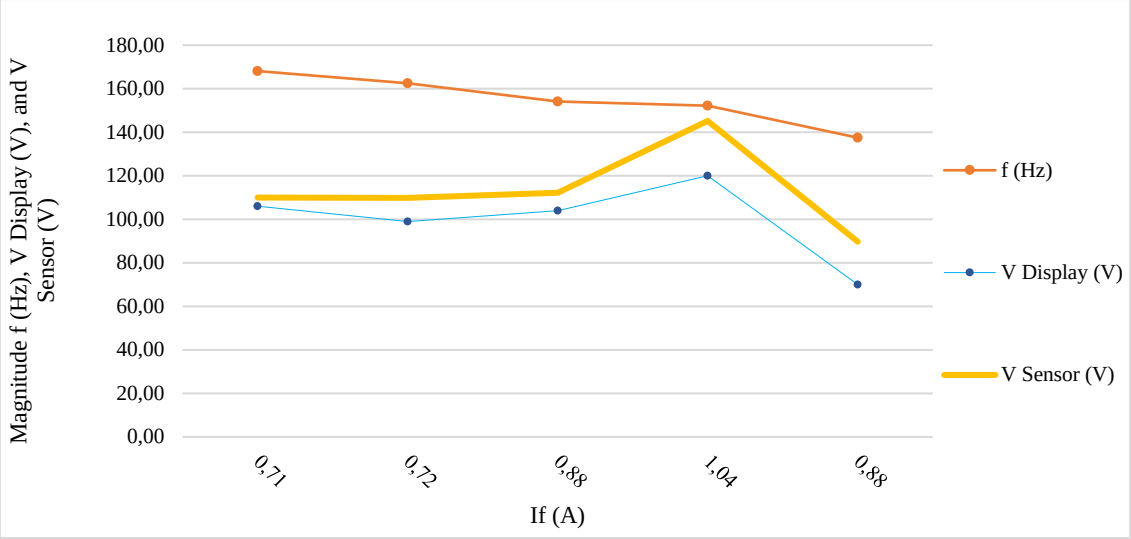

Figure 21. Graph of the effect I_f against V_{out} and f.

4. Conclusion

Based on system testing carried out using the P, PI, and PID methods, the best control method was obtained with a E_{ss} (steady-state error) of 0%, M_p (maximum overshoot) of 4.7%, and T_r (rise time) of 4.965 s using the PI control method. Comparison of the response of the simulation results with direct testing of the tool, it is found that the response time in the tool test is faster than the simulation, and the maximum overshoot and steady-state error is greater in the tool test than the simulation. The effect of using PI control with the response characteristics of the tool T_r = 1.9 s, T_s = 6.6 s, M_p = 38.95%, and E_{ss} = 11.02%, on the generator excitation current will increase in line with the increase in load current, while for The resulting generator output voltage will be stable due to the increase in excitation current with an error that occurs when compared to the nominal working voltage of 10.51%. A large error occurs because the resulting frequency does not match the nominal working frequency so that the sensor reads an error.

References

[1] Suharyati, S. H. Pambudi, J. L. Wibowo, and N. I. Pratiwi, *Indonesia Energy Outlook 2019*. Jakarta, Indonesia: Secretariat General of the National Energy Council, Sep. 2019.

[2] I. Boldea, *Electric Generators Handbook: Synchronous Generators*, 2nd ed. Florida, USA: CRC Press, Sep. 2015.

[3] Y. A. Ahmed, Y. I. Al-Mashhadany, and M. A. Nayyef, "High performance of excitation system for synchronous generator based on modeling analysis," *Bull. Electr. Eng. Inform.*, vol. 9, no. 6, pp. 2235–2243, Dec. 2020, doi: 10.11591/eei.v9i6.2627.

[4] J. Li, *Design and Application of Modern Synchronous Generator Excitation Systems*. Singapore: John Wiley & Sons, 2019.

[5] D. Jiang *et al.*, "Research on excitation system of synchronous generator," *J. Phys.: Conf. Ser.*, vol. 1607, no. 1, p. 012040, Aug. 2020, doi: 10.1088/1742-6596/1607/1/012040.

[6] A. A. Bhutto, F. A. Chachar, M. Hussain, D. K. Bhutto, and S. E. Bakhsh, "Implementation of probabilistic neural network (PNN) based automatic voltage regulator (AVR) for excitation control system in Matlab," in *2019 2nd Int. Conf. Comput. Math. Eng. Technol. (iCoMET)*, Sukkur, Pakistan, Mar. 2019, pp. 1–5, doi: 10.1109/ICOMET.2019.8673416.

[7] D. W. Pribadi, E. Wahjono, and I. Ferdiansyah, "Optimizing of synchronous generator voltage stability with CUK converter as an excitation control system," in *2020 Int. Conf. Electr. Eng. Inform. (ICELTICs)*, Aceh, Indonesia, Oct. 2020, pp. 1–6, doi: 10.1109/ICELTICs50595.2020.9315443.

[8] A. M. Hemeida *et al.*, "TCSC with auxiliary controls based voltage and reactive power controls on grid power system," *Ain Shams Eng. J.*, vol. 11, no. 3, pp. 587–609, Sep. 2020, doi: 10.1016/j.asej.2019.10.015.

[9] A. T. N. Angga *et al.*, "Use Of ACS 712ELC-5A current sensor on overloaded load installation safety system," *Appl. Technol. Comput. Sci. J.*, vol. 4, no. 1, pp. 47–55, Jul. 2021, doi: 10.33086/atcsj.v4i1.2088.

[10] M. S. Fahmi and Irwanto, "Supplay eksitasi output generator 300 Mw menggunakan metode pola titik daya reaktif," *J. Tek. Mesin Mekatronika (J. Mech. Eng. Mechatron.)*, vol. 5, no. 1, pp. 11–20, Apr. 2020, doi: 10.33021/jmem.v5i1.983.

[11] E. C. Lister, *Mesin dan Rangkaian Listrik*, 6th ed. Jakarta, Indonesia: Erlangga, 1998.

[12] A. T. Nugraha and D. Priyambodo, "Prototype hybrid power plant of solar panel and vertical wind turbine as a provider of alternative electrical energy at Kenjeran beach Surabaya," *J. Electr., Electromed. Eng. Med. Inform.*, vol. 2, no. 3, pp. 108–113, Oct. 2020, doi: 10.35882/jeeemi. v2i3.4.

[13] D. Dewatama, M. Fauziah, and K. H. Safitri, "Kendali DC-DC converter pada portable pico-hydro menggunakan PID kontroller," *J. Eltek*, vol. 16, no. 2, pp. 113–124, Oct. 2018, doi: 10.33795/eltek.v16i2.103.

[14] A. T. Nugraha, M. Z. A. Tiwana, and A. M. Ravi, "Analisis optimalisasi manajemen daya chiller untuk rencana AC sentral industri," *J. Janitra Inform. Sist. Inf.*, vol. 1, no. 1, pp. 35–46, Apr. 2021, doi: 10.25008/janitra.v1i1.106.

[15] L. Ljung, A. A. Ozdemir, and R. Singh, "Online features in the MATLAB® system identification ToolboxTM," *IFAC-PapersOnLine*, vol. 51, no. 15, pp. 700–705, Jul. 2018, doi: 10.1016/j.ifacol. 2018.09.201.

[16] T. D. Pamungkas, U. Sutisna, and Y. R. Fauzan, "Penerapan algoritma fuzzy untuk optimasi kontroler PID pada sistem kontrol AVR generator 3 fasa 480VA berbasis mikrokontroler ATMega16," *Iteks*, vol. 10, no. 2, Nov. 2018.

[17] L. Ljung, C. Andersson, K. Tiels, and T. B. Schön, "Deep learning and system identification," *IFAC-PapersOnLine*, vol. 53, no. 2, pp. 1175–1181, Jul. 2020, doi: 10.1016/j.ifacol.2020.12.1329.

[18] Y. Naung, A. Schagin, H. L. Oo, K. Z. Ye, and M. Z. Khaing, "Implementation of data driven control system of DC motor by using system identification process," in *2018 IEEE Conf. Rus. Young Res. Electr. Electron. Eng. (EIConRus)*, Moscow and St. Petersburg, Russia, Jan. 2018, pp. 1801–1804, doi: 10.1109/EIConRus.2018.8317455.

[19] K. Ogata and E. Leksono, *Teknik Kontrol Automatik (Sistem Pengaturan)*. Jakarta, Indonesia: Erlangga, 1995.

[20] F. Asadi, R. E. Bolanos, and J. Rodríguez, *Feedback Control Systems: The MATLAB®/Simulink® Approach*. Switzerland: Springer Nature, 2022.